Influence of substrate tilt angle on the incorporation of $BaHfO_3$ in thick $YBa_2Cu_3O_{7-\delta}$ films

Reference:

Sieger Max, Pahlke Patrick, Ottolinger Rick, Meledin Alexander, Van Tendeloo Gustaaf, et al..- Influence of substrate tilt angle on the incorporation of $BaHfO_3$ in thick $YBa_2Cu_3O_{7-\delta}$ films
IEEE transactions on applied superconductivity / IEEE [New York, N.Y.] - ISSN 1051-8223 - (2016), p. 1-4
Full text (Publishers DOI): http://dx.doi.org/doi:10.1109/TASC.2016.2631587

Influence of substrate tilt angle on the incorporation of $BaHfO_3$ in thick $YBa_2Cu_3O_{7-\delta}$ films

Journal:	*Applied Superconductivity Conference 2016*
Manuscript ID	Draft
Conference Manuscript Type:	Contributed Manuscript
Date Submitted by the Author:	n/a
Complete List of Authors:	Sieger, Max; Leibniz Institute for Solid State and Materials R, Functional Oxide Layers and Superconductors Group Pahlke, Patrick; IFW Dresden, Functional Oxide Layers and Superconductors Group Ottolinger, RIck; Leibniz Institute for Solid State and Materials R, Functional Oxide Layers and Superconductors Group STAFFORD, Benjamin; THEVA Dünnschichttechnik GmbH, Research & Development; Leibniz-Institute for Solid State and Materials Research, Institute for Metallic Materials LAO, Mayraluna MELEDIN, Alexander Bauer, Markus; Theva Dünnschichttechnik GMBH, . Eisterer, Michael; Vienna University of Technology, Van Tendeloo, Gustaaf; University of Antwerp, Schultz, L.; Leibniz Institute for Solid State and Materials R Nielsch, Kornelius; IFW Dresden, Institute for Metallic Materials Hühne, Ruben; IFW Dresden
Keywords:	Cuprates < Materials, Critical current and flux pinning < Properties, Critical current measurement < Critical current and flux pinning < Properties, 2G HTS Conductors < Coated conductors < Conductors, Thick films < Thin films and multilayers < Materials, Templates < Coated conductors < Conductors

Influence of substrate tilt angle on the incorporation of $BaHfO_3$ in thick $YBa_2Cu_3O_{7-\delta}$ films

Max Sieger, Patrick Pahlke, Rick Ottolinger, Benjamin H. Stafford, Mayraluna Lao, Alexander Meledin, Markus Bauer, Michael Eisterer, Gustaaf Van Tendeloo, Ludwig Schultz, Kornelius Nielsch, Ruben Hühne

Abstract— **High critical current densities can be realized in high-temperature superconductors such as $YBa_2Cu_3O_{7-\delta}$ (YBCO) by controlling density, shape, size and direction of a secondary phase. Whereas the dependence on the growth rate and deposition temperature has been widely studied as key parameters for nano-engineering the pinning landscape, the vicinal tilt of the substrate surface might have an additional influence. Therefore, we deposited 6 mol% $BaHfO_3$ (BHO) doped YBCO on $SrTiO_3$ (STO) substrates with vicinal angles α between 0° and 40° to identify the influence of the tilt on the growth mode of BHO. An undisturbed epitaxial growth of the superconductor as well as an epitaxial integration of the BHO phase in the YBCO matrix is observed for all vicinal angles investigated. The critical temperature is constant up to $\alpha = 20°$, whereas the self-field critical current density at 77 K starts to decrease above 10°. A detailed structural analysis of the film cross sections showed that the growth mode of BHO changes already for a vicinal tilt of 2° from a pure *c*-axis oriented growth to a layered structure with BHO aligned parallel to the YBCO *ab*-plane. We identified a strong influence of such a microstructure on the current flow in BHO doped YBCO films on STO substrates as well as on MgO based coated conductors prepared by inclined substrate deposition.**

Index Terms— **BHO, pinning, pulsed laser deposition, ISD, vicinal angle, YBCO**

I. Introduction

NANO-ENGINEERING the density, shape, size and alignment of artificial pinning centers is a key technology to achieve high critical current densities (J_c) in $YBa_2Cu_3O_{7-\delta}$ (YBCO)-based coated conductors in medium and high-magnetic fields [1]. We have realized self-assembled $BaHfO_3$ (BHO) nanocolumns oriented parallel to the *c*-axis in thick YBCO films on technical Ni-W RABiT substrates [2],[3] as well as on IBAD-YSZ textured tapes [4] with improved in-field performance for $B \| c_{YBCO}$. Here, length, dimension and splay of the nanoprecipitates can be tailored by careful adjustment of key parameters such as growth rate (R), deposition temperature (T_S) and doping level [5]. In contrast, it is challenging to grow self-assembled nanocolumns in doped YBCO films on inclined substrate deposition (ISD)-MgO buffered tape. So far, no *c*-axis correlated defects are achieved, i.e. no $B \| c$ peak appears in angle-dependent J_c measurements of such samples [6]. TEM investigations show the formation of alternating YBCO layers and BHO/Y_2O_3 platelets which are aligned parallel the YBCO *ab*-plane [5],[6].

In this work, we studied the influence of the vicinal angle α of miscut $SrTiO_3$ (mSTO) single crystal substrates on the growth mode of nanosized BHO structures in thick YBCO films. The layers on mSTO act as a model system for BHO doped YBCO films on different technical substrates: low vicinal angles can represent slightly tilted (<10°) single grains on RABiTS Ni-W, whereas high α describe the situation of ISD-MgO layers with an inclination of about 30°.

II. Experimental Details

A. Sample preparation

We prepared about 1 µm thick YBCO films with additional 6 mol% BHO (BHO:YBCO) by pulsed laser deposition (PLD) from premixed targets utilizing a Lambda Physics LPX305Pro KrF excimer laser ($\lambda = 248$ nm) with an energy density of 1.6 J/cm² at the target surface and a pulse frequency of 10 Hz (i.e. growth rate ~1 nm/s). The films were grown on vicinal $SrTiO_3$ substrates with α being the angle between the [001] direction and the substrate normal ranging from 0° to 40°. All films were deposited at 0.4 mbar oxygen partial pressure and 830°C substrate temperature and annealed in 400 mbar O_2 at 765°C for one hour. For comparison, a YBCO film with similar thickness but 5 mol% BHO addition was prepared on a ISD-MgO buffered Hastelloy tape having a 300 nm thin $GdBa_2Cu_3O_7$ seed layer. All films were covered with a silver cap layer to protect the sample surface and lower the contact resistance for electric measurements.

B. Structural characterization

Secondary electron images of the samples surfaces were taken on a *LEO Gemini 1530* operated at 20 kV. Focused Gallium ion beam cuts were carried out parallel to both sample axes on a *FEI Helios Nanolab 600i* to analyze film thickness, tilt and shape of the secondary phases. High-angle annular dark field scanning transmission electron microscopy (HAADF-STEM), annular dark field scanning transmission

---

This work was supported by EUROTAPES, a collaborative project funded by the European Commission's Seventh Framework Program (FP7 / 2007 - 2013) under Grant Agreement n.280432. (Corresponding author: M. Sieger)

M. Sieger, P. Pahlke, R. Ottolinger, K. Nielsch and L. Schultz are with IFW Dresden, 01069 Dresden, Germany and also with Dresden University of Technology, 01062 Dresden, Germany (e-mail: m.sieger@ifw-dresden.de).

B. H. Stafford is with THEVA Dünnschichttechnik GmbH, 85737 Ismaning, Germany, IFW Dresden, 01069 Dresden, Germany and also with Dresden University of Technology, 01062 Dresden, Germany (e-mail: stafford@theva.com).

M. Lao and M. Eisterer are with Atominstitut, TU Wien, 1020 Vienna, Austria (e-mail: michael.eisterer@tuwien.ac.at).

A. Meledin and G. V. Tendeloo are with Electron microscopy for materials science (EMAT), University of Antwerp, 2020 Antwerp, Belgium (e-mail: staf.vantendeloo@uantwerpen.be).

M. Bauer is with THEVA Dünnschichttechnik GmbH, 85737 Ismaning, Germany (e-mail: bauer@theva.com).

R. Hühne is with IFW Dresden, 01069 Dresden, Germany (e-mail: R.Huehne@ifw-dresden.de).

electron microscopy (ADF-STEM) and energy dispersive X-Ray spectroscopy (EDX) mappings were performed on an *FEI Tecnai Osiris* microscope operated at 200 kV as well as on an *FEI Titan* “cubed” electron microscope operated at 200 kV and 300 kV. X-Ray diffraction (XRD) patterns were measured on a Philips X’Pert PW3040 diffractometer using a Cu anode. The *c*-axis parameter of YBCO was calculated from peak positions of the (00ℓ) peaks.

C. *Electrical properties*

The critical temperature $T_{c,50}$ and the transition width ΔT_c (= $T_{c,90}$ - $T_{c,10}$) were measured inductively. Trapped field profile measurements by scanning Hall probe microscopy (SHPM) were carried out to determine the local distribution of the critical current. For the detailed procedure see Ref. [7].

III. RESULTS AND DISCUSSION

A. *Structural properties*

The epitaxial growth of the BHO:YBCO layers on the vicinal substrates was verified by X-Ray diffraction. The XRD patterns of the films are shown in Fig. 1 indicating a strong *c*-axis-oriented growth of the superconductor by the appearance of strong (00ℓ) peaks even at high vicinal angles. The peaks broaden with increasing vicinal angle (full width at half maximum for YBCO (005): 0.29° for α=0°, 0.67° for α=40°), whereas the *c*-axis parameter decreases almost linearly from 11.83 Å for α=0° to 11.73 Å for α=40°. The BHO (400) and Y_2O_3 (400) peaks are shifted from their theoretical position and have an non-symmetrical shape, which might be explained by the incorporation of Y in BHO or Hf in Y_2O_3, respectively [3],[5],[8]. For the sample on the 30° tilted ISD-MgO template, the BHO peak is overlapped by the strong MgO (200) buffer layer peak. Also in this case, an *a*-axis peak is apparent. Pole figure measurements (not shown here) indicate that BHO and Y_2O_3 are incorporated epitaxially with a cube-on-cube relationship.

The surface morphology of the BHO:YBCO films on mSTO substrates with high vicinal angles (α ≥ 10°) is different from similar films on flat surfaces. Top-view SEM images (Fig. 2) show a terrace structure evolving with increasing vicinal angle. Exceeding a critical angle of α~20°, cracks appear at the film surface (Fig. 2(f)) possibly due to the relaxation of stresses inside the films. A quasi-3D representation of the BHO:YBCO film on 25° mSTO shows stacked planes of YBCO and secondary phases (Fig. 3) leading to the observed surface terraces. Whereas YBCO forms closed layers, the secondary phases of BHO/Y_2O_3 type are elongated in *ab*-direction but do not develop continuous layers. A similar situation is found in BHO:YBCO films on ISD-MgO-buffered Hastelloy tape (α~30°). The tilted template leads to a terraced surface with a step width of ~150 nm (Fig. 4(a)). The cross-section view (Fig. 4(b)) is almost similar to the BHO:YBCO layer on 25° mSTO (Fig. 3).

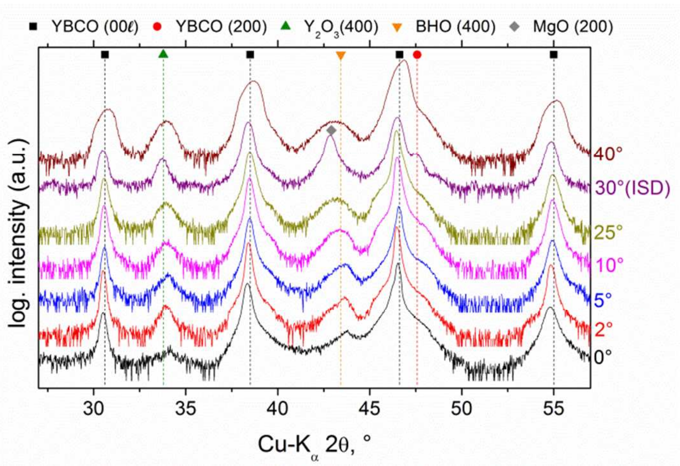

Fig. 1. XRD pattern of BHO:YBCO films on mSTO substrates with different vicinal angles α = 0 to 40° and a similar film on ISD-MgO buffered Hastelloy (dashed lines indicate theoretical peak positions).

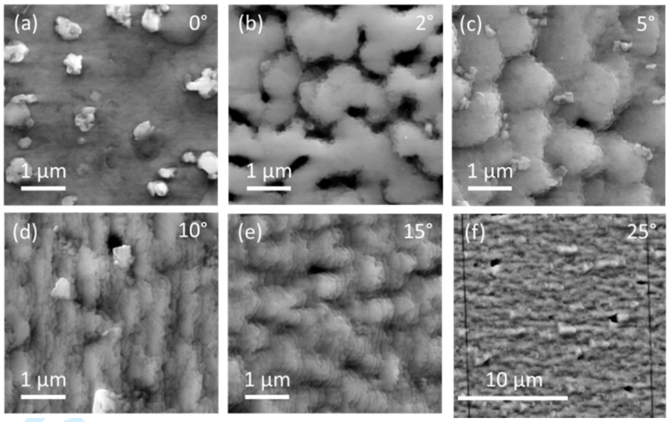

Fig. 2. Secondary electron images of BHO:YBCO films on mSTO substrates with vicinal angles α of 0° (a), 2° (b), 5° (c), 10° (d),15° (e) and 25° (f). Cracks are apparent in (f).

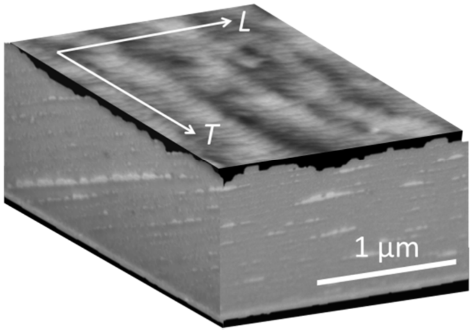

Fig. 3. Quasi-3D visualization by combined top-view and side-view SEM of the BHO:YBCO film on 25° vicinal STO. *L* and *T* denote the longitudinal and transversal directions of the J_c mappings (cf. Fig. 7).

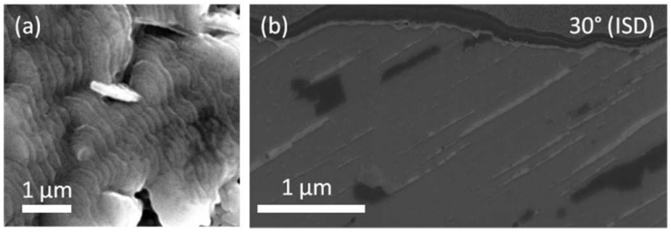

Fig. 4. Top-view (a) and side-view (b) SEM of the BHO:YBCO layer on GdBCO-buffered ISD-MgO/Hastelloy tape.

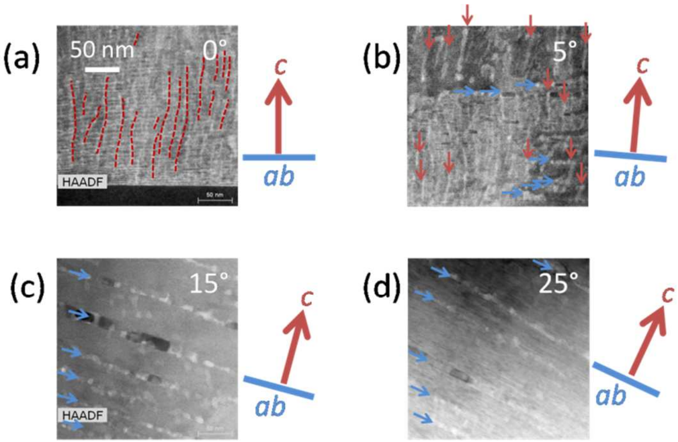

Fig. 5. HAADF-STEM images of BHO:YBCO films on highly-oriented STO (α = 0°) showing *c*-axis-aligned nanorods (red) (a), low-angle mSTO (α = 5°) showing a mix of *c*-axis-aligned nanorods containing Hf and *ab*-plane-parallel platelets of BHO/Y_2O_3 (blue) (b), and high-angle mSTO (α = 15° / 25°) showing platelets parallel to the *ab*-plane only (c),(d).

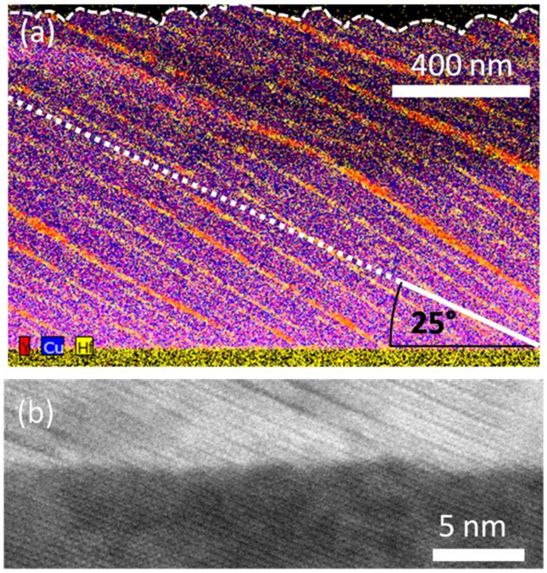

Fig. 6. BHO:YBCO film on mSTO (α=25°): STEM-EDX composite map for Y, Cu and Hf, surface roughness and substrate vicinal angle marked by white dashed lines (a) and ADF-STEM image of the YBCO/STO interface (b).

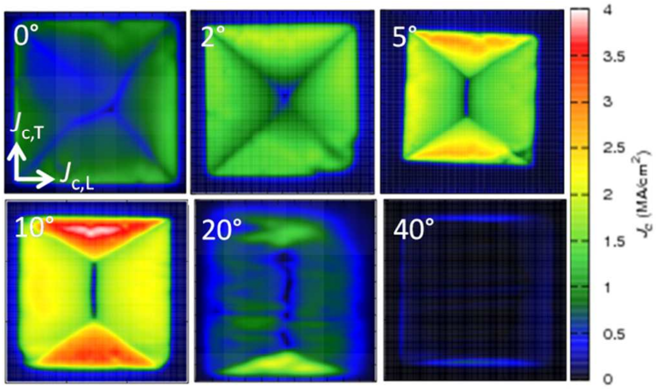

Fig. 7. Spatial J_c distribution evaluated from SHPM images of 6 mol% BHO:YBCO films on mSTO substrates at 77 K, self-field.

The surface roughness is decreased for both substrates compared to pristine YBCO films. BHO addition seems to prevent the formation of large Y_2O_3 agglomerates, which act as nucleation centers for pores as shown previously for BHO:YBCO films on Ni-W tapes [3] as well as on ABAD-YSZ buffered templates [4].

STEM images from BHO:YBCO films on a highly-oriented STO (α = 0°, Fig. 5(a)) and mSTO substrates with small (α = 5°, Fig. 5(b)) and high miscut (α = 15° and 25° respectively, Fig. 5(c)+(d)) indicate the influence of the tilt on the local microstructure resulting in a change from *c*-axis parallel nanorods to *ab*-planar structures with increasing vicinal angle. Whereas structures parallel to the *c*-axis are only formed on flat surfaces (similar to ABAD-YSZ-buffered templates in [5]), a mixed microstructure containing short columns parallel to c_{YBCO} as well as planes parallel to the *ab*-plane are formed for α = 2 to 5°. With higher tilt, the columns disappear and tilted platelets are the predominant form of secondary phases as observed for the highly tilted films on ISD-tapes (cf. Fig. 9 in [5]). The formation of planar stacks of pure YBCO layers and secondary phases might be induced by changes in growth mode. A possible origin for a planar growth might be the faster diffusion of particles along ab_{YBCO} compared to c_{YBCO} during deposition, which leads to a higher growth velocity along the tilted planes.

The tilt angle of single platelets is not always in accordance with the vicinal angle as exemplary shown for the BHO:YBCO film with α = 25° in Fig. 6(a). Discrete kinks can be found as well as curved segments. Further detailed studies are required to evaluate their origin. Plane buckling and tilting is already apparent at the YBCO/STO interface (Fig. 6(b)), but with a much lower roughness compared to the film top surface (white dashed line in Fig. 6(a)).

B. Electrical properties

The lamellar growth of BHO:YBCO films on highly-tilted surfaces leads to a highly anisotropic J_c behavior. Figure 7 gives J_c mappings evaluated from the trapped field profiles. Here $J_{c,L}$ (longitudinal) and $J_{c,T}$ (transversal) denote the critical current density parallel and perpendicular (across the *ab*-planes) to the surface terraces respectively, as depicted in Fig. 3. The smaller absolute values of J_c for the films with low vicinal angles (α = 0 to 5°) are related to the T_c values: The BHO:YBCO film on 10° mSTO has the highest $T_{c,50}$ (89.2 K) and smallest transition width ΔT_c (0.4 K) compared to the film on highly-oriented STO (84.9 K / 1.5 K) and on 2° mSTO (88.6 K / 0.6 K). Whereas the film on highly-oriented STO exhibits almost no anisotropy, i.e. $J_{c,L} / J_{c,T} \sim 1$, the samples on 2° (1.24), 5° (1.38) and 10° mSTO (1.64) show an increasing anisotropy with increasing vicinal angle. An explanation for the increasing anisotropy is given by Lao et al.: The tilted BHO/Y_2O_3 planes act as elements blocking the current that leads to a smaller conducting volume the steeper the vicinal angle gets [9]. The J_c mappig for the BHO:YBCO film on 20° and 45° mSTO have a filamentary structure originating from the observed cracks in this films (cf. Fig. 1(f)).

IV. CONCLUSION

We deposited BHO doped YBCO films on miscut STO single crystals and found that the vicinal angle α of the substrate has a significant influence on the pinning landscapes. Highly oriented surfaces ($\alpha = 0°$) lead to *c*-axis-oriented BHO columns, similar to BHO:YBCO films on ABAD-YSZ buffered templates, which exhibit only very small angular deviations in the textured buffer layer. Low miscut angles ($\alpha = 2$ to $10°$) lead to the formation of a mixed structure containing *c*-axis-oriented columns and *ab*-parallel planes. Higher vicinal angles ($\alpha > 10°$) lead to pure planar stacking of YBCO planes as well as intermixed BHO and Y_2O_3 platelets. A similar structure is observed in BHO:YBCO films on ISD-MgO buffered templates that have an inclination of ~30°. J_c mappings revealed that the anisotropy (longitudinal versus transversal critical current density) increases with α as BHO/Y_2O_3 layers block the current in the transverse direction. For very high $\alpha \geq 20°$ cracks evolve parallel the surface terraces blocking the current transport completely.

ACKNOWLEDGMENT

The authors would like to thank R. Nast, M. Reitner, M. Kühnel, U. Fiedler and J. Scheiter for technical assistance.

REFERENCES

[1] B. Maiorov, S. A. Baily, H. Zhou, O. Ugurlu, J. A. Kennison, P. C. Dowden, T. G. Holesinger, S. R. Foltyn and L. Civale, “Synergetic combination of different types of defect to optimize pinning landscape using $BaZrO_3$-doped $YBa_2Cu_3O_7$”, APL, Vol. 8, 398-404, May 2009.

[2] M. Sieger, J. Hänisch, K. Iida, U. Gaitzsch, C. Rodig, L. Schultz, B. Holzapfel and R. Hühne, “Pulsed laser deposition of thick $BaHfO_3$-doped $YBa_2Cu_3O_{7-\delta}$ films on highly alloyed textured Ni-W tapes”, *J. Phys.: Conf. Ser.*, vol. 507, Art. No. 022032, 2014.

[3] M. Sieger, J. Hänisch, P. Pahlke, M. Sparing, U. Gaitzsch, K. Iida, R. Nast, E. Reich, L. Schultz, B. Holzapfel and R. Hühne, “$BaHfO_3$-doped thick $YBa_2Cu_3O_{7-\delta}$ films on highly alloyed textured Ni-W tapes”, *IEEE Trans. Appl. Supercond.*, vol. 25, no. 3, Art. No. 6602604, 2014.

[4] P. Pahlke, M. Lao, M. Eisterer, A. Meledin, G. Van Tendeloo, J. Hänisch, M. Sieger, A. Usoskin, J. Strömer, B. Holzapfel, L. Schultz and R. Hühne, “Reduced J_c anisotropy and enhanced in-field performance in thick $BaHfO_3$- doped $YBa_2Cu_3O_{7-\delta}$ films on ABAD-YSZ templates”, *IEEE Trans. Appl. Supercond*., vol. 26, no. 3, Art. No. 6603104, March 2016.

[5] M. Sieger, P. Pahlke, M. Lao, M. Eisterer, A. Meledin, G. Van Tendeloo, R. Ottolinger, J. Hänisch, B. Holzapfel, A. Usoskin, A. Kursomovic, J. MacManus-Driscoll, B. H. Stafford, M. Bauer, K. Nielsch, L. Schultz and R. Hühne, “Tailoring microstructure and superconducting properties in thick $BaHfO_3$ and $Ba_2Y(Nb/Ta)O_6$ doped YBCO films on technical substrates”, *IEEE Trans. Appl. Supercond.*, submitted for pbulication.

[6] B. Stafford, M. Sieger, O. Troshyn, R. Nast, M. Döblinger, R. Hühne, M. Bauer, B. Holzapfel and L. Schultz, “Pinning Centres in ISD-MgO Coated Conductors via EBPVD”, *IEEE Trans. Appl. Supercond.*, vol. 26, no. 3, Art. No. 6601105, 2016.

[7] F. Hengstberger, M. Eisterer, M. Zehetmayer and H. W. Weber, “Assessing the spatial and field dependence of the critical current density in YBCO bulk superconductors by scanning Hall probes“, *Supercond. Sci. Technol.,* Vol. 22, Art. No. 025011, January 2009.

[8] E. Reich, T. Thersleff, R. Hühne, K. Iida, L. Schultz and B. Holzapfel, "Structural and pinning properties of $Y_2Ba_4CuMO_y$ (M = Nb, Zr)/$YBa_2Cu_3O_{7-\delta}$ quasi-multilayers fabricated by off-axis pulsed laser deposition", *Supercond. Sci. Technol.*, Vol. 22, Art. No. 105004, Aug. 2009.

[9] M. Lao, J. Hecher, M. Sieger, P. Pahlke, M. Bauer, R. Hühne and M. Eisterer, “Advanced scanning Hall probe microscopy: assessing anisotropy and field dependence of J_c in the low limit”, *Supercond. Sc. Tech. - Focus issue on magnetic properties of superconductors*, submitted for publication.